Author(s): Tuovinen, Toni & Hinkkanen, Marko & Luomi, Jorma

Title: Modeling of Mutual Saturation in Induction Machines

Year: 2008

Version: Post print

Please cite the original version:

Tuovinen, Toni & Hinkkanen, Marko & Luomi, Jorma. 2008. Modeling of Mutual Saturation in Induction Machines. 2008 IEEE Industry Applications Society Annual Meeting. 8. ISBN 978-1-4244-2279-1 (electronic). DOI: 10.1109/08ias.2008.32.

Modeling of Mutual Saturation in Induction Machines

Toni Tuovinen, Marko Hinkkanen, and Jorma Luomi
Department of Electrical Engineering
Helsinki University of Technology
P.O. Box 3000, FI-02015 TKK, Finland

***Abstract*—Mutual saturation between the main flux and the rotor leakage flux appears in induction machines, especially if the rotor slots are skewed or closed. Conventional saturation models used in connection with dynamic equivalent-circuit models do not take this phenomenon into account. In this paper, explicit functions for modeling the mutual saturation are proposed. The proposed functions are physically reasonable, they are easy to fit, and the number of their parameters is small. The proposed functions can be used in real-time applications and in computer simulations where high accuracy and physical consistency are preferable. The model fits well to the data obtained from finite element analysis or experimental data of a 2.2-kW motor.**

***Index Terms*—Induction motors, motor models, mutual saturation, closed slots, rotor skew.**

I. Introduction

Induction machines are usually magnetically saturated in the rated operating point. The main flux saturates strongly as a function of the magnetizing current. Furthermore, it has been observed that the main flux may depend significantly on the load (or the rotor current) [1], [2]. This mutual saturation effect originates mainly from skewed and closed rotor slots [3], which are used in the majority of small machines. A typical main-flux saturation characteristics is sketched in Fig. 1; to model the inductance corresponding to the figure, a function of two variables (i.e. a surface) is needed.

If the geometry of the machine and the material properties are known, magnetic saturation can be modeled with good accuracy using finite-element analysis (FEA) [4]. However, FEA is computationally too demanding for many applications, including real-time flux estimation in controlled drives, design of control algorithms, and simulations of transient phenomena. Instead, models based on lumped parameters, such as the equivalent circuit in Fig. 2, are commonly used.

In equivalent-circuit models, the magnetizing inductance is usually assumed to saturate only as a function of the magnetizing current or main flux [5], [6], [7]. The leakage inductances have been modeled as functions of their own currents [5], [8]. For the magnetizing curve, explicit functions have been used, e.g. polynomials [9], [7], power functions [10], [5], and rational power functions [11]. In these previously proposed models, the mutual saturation effect is omitted. The small-signal model proposed in [12] takes the mutual saturation effect into account, but no explicit functions are given for saturation characteristics.

If high accuracy is required, conventional saturation models used in connection with equivalent-circuit models may not be sufficient. In controlled drives, for example, an oversimplified saturation model may result in poor accuracy of the produced torque or even instability in speed-sensorless drives.

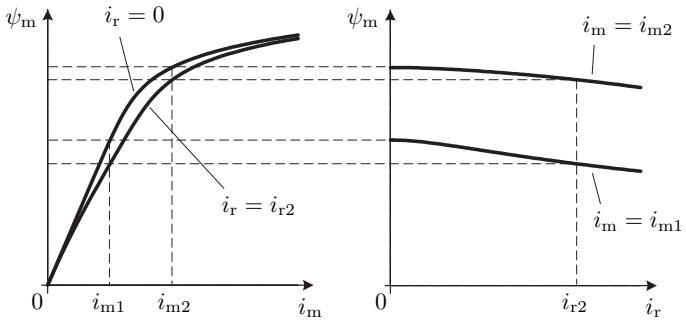

Fig. 1. Typical saturation characteristics of main flux $\psi_\mathrm{m}(i_\mathrm{m}, i_\mathrm{r})$. On the left-hand side, ψ_m is shown as a function of magnetizing current i_m for two different values of rotor current ($i_\mathrm{r}=0$ corresponding to no-load operation and i_r2 corresponding to constant rotor current). On the right-hand side, ψ_m is shown as a function of i_r for two values of i_m.

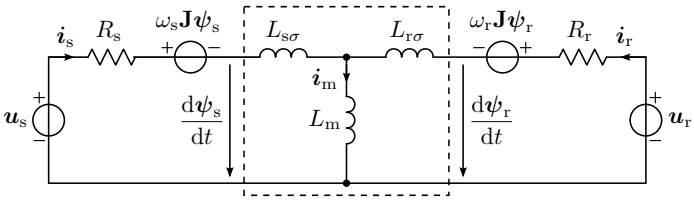

Fig. 2. Dynamic T model of an induction motor in coordinates rotating at angular speed ω_s, the angular slip frequency being ω_r. The magnetic circuit (dashed line) is assumed to be lossless.

The inductance values of a machine cannot be measured directly. Usually, only the stator current, the stator voltage and the rotor speed are measured. If the magnetic saturation is modeled using functions, it is possible to obtain the function parameters by exploiting experimental data from several operating points [13].

In this paper, explicit functions are proposed for the saturation characteristics—including the mutual saturation. The inductances become functions of two variables (fluxes or currents). The proposed functions are physically reasonable, they are easy to fit, and the number of parameters is comparatively small. The proposed functions can be used in computer simulations where high accuracy and physical consistency are preferable. As an example, the inductance data of a 2.2-kW induction motor (obtained from FEA) are fitted to the proposed model, and a method to obtain the model parameters from laboratory measurements is demonstrated.

II. Machine Model

Vectors will be denoted by boldface lowercase letters and matrices by boldface uppercase letters. The matrix transpose will be marked with the superscript T. The identity matrix, the orthogonal rotation matrix, and the zero matrix are

$$\mathbf{I} = \begin{bmatrix} 1 & 0 \\ 0 & 1 \end{bmatrix}, \quad \mathbf{J} = \begin{bmatrix} 0 & -1 \\ 1 & 0 \end{bmatrix}, \quad \mathbf{0} = \begin{bmatrix} 0 & 0 \\ 0 & 0 \end{bmatrix} \tag{1}$$

respectively.

In a synchronous coordinate system rotating at angular speed ω_s, the voltage equations of the induction machine are

$$\frac{\mathrm{d}\boldsymbol{\psi}_\mathrm{s}}{\mathrm{d}t} = \boldsymbol{u}_\mathrm{s} - R_\mathrm{s}\boldsymbol{i}_\mathrm{s} - \omega_\mathrm{s}\mathbf{J}\boldsymbol{\psi}_\mathrm{s} \tag{2a}$$

$$\frac{\mathrm{d}\boldsymbol{\psi}_\mathrm{r}}{\mathrm{d}t} = \boldsymbol{u}_\mathrm{r} - R_\mathrm{r}\boldsymbol{i}_\mathrm{r} - \omega_\mathrm{r}\mathbf{J}\boldsymbol{\psi}_\mathrm{r} \tag{2b}$$

where $\boldsymbol{u}_\mathrm{s} = [u_\mathrm{sd}, u_\mathrm{sq}]^\mathrm{T}$ is the stator voltage vector, $\boldsymbol{i}_\mathrm{s} = [i_\mathrm{sd}, i_\mathrm{sq}]^\mathrm{T}$ the stator current vector, and R_s the stator resistance. The rotor resistance is R_r, the rotor voltage vector $\boldsymbol{u}_\mathrm{r}$, the rotor current vector $\boldsymbol{i}_\mathrm{r}$, and the angular slip frequency $\omega_\mathrm{r} = \omega_\mathrm{s} - \omega_\mathrm{m}$, the electrical angular speed of the rotor being ω_m. A short-circuited rotor winding will be considered in this paper, i.e. $\boldsymbol{u}_\mathrm{r} = [0, 0]^\mathrm{T}$.

The stator and rotor flux linkage vectors are

$$\boldsymbol{\psi}_\mathrm{s} = L_\mathrm{s}\boldsymbol{i}_\mathrm{s} + L_\mathrm{m}\boldsymbol{i}_\mathrm{r} \tag{3a}$$

$$\boldsymbol{\psi}_\mathrm{r} = L_\mathrm{m}\boldsymbol{i}_\mathrm{s} + L_\mathrm{r}\boldsymbol{i}_\mathrm{r} \tag{3b}$$

respectively, where L_m is the magnetizing inductance. The stator and rotor inductances are defined by $L_\mathrm{s} = L_\mathrm{m} + L_{\mathrm{s}\sigma}$ and $L_\mathrm{r} = L_\mathrm{m} + L_{\mathrm{r}\sigma}$, respectively, where $L_{\mathrm{s}\sigma}$ and $L_{\mathrm{r}\sigma}$ are the stator and rotor leakage inductances, respectively. The T-equivalent circuit model corresponding to (2) and (3) is depicted in Fig. 2. The stator and rotor leakage fluxes are $\boldsymbol{\psi}_{\mathrm{s}\sigma} = L_{\mathrm{s}\sigma}\boldsymbol{i}_\mathrm{s}$ and $\boldsymbol{\psi}_{\mathrm{r}\sigma} = L_{\mathrm{r}\sigma}\boldsymbol{i}_\mathrm{r}$, respectively, and the main flux is $\boldsymbol{\psi}_\mathrm{m} = L_\mathrm{m}\boldsymbol{i}_\mathrm{m}$, where $\boldsymbol{i}_\mathrm{m} = \boldsymbol{i}_\mathrm{s} + \boldsymbol{i}_\mathrm{r}$ is the magnetizing current.

It is worth noticing that the flux vectors are assumed to be parallel with the corresponding current vectors in accordance with Fig. 2, while the scalar-valued inductances may be functions of the currents or fluxes. All inductances are assumed to be lossless. Hence, the inductances should fulfill the reciprocity conditions [14], [3]:

$$\frac{\partial\psi_\mathrm{m}}{\partial i_\mathrm{s}} = \frac{\partial\psi_{\mathrm{s}\sigma}}{\partial i_\mathrm{m}}, \quad \frac{\partial\psi_\mathrm{m}}{\partial i_\mathrm{r}} = \frac{\partial\psi_{\mathrm{r}\sigma}}{\partial i_\mathrm{m}}, \quad \frac{\partial\psi_{\mathrm{r}\sigma}}{\partial i_\mathrm{s}} = \frac{\partial\psi_{\mathrm{s}\sigma}}{\partial i_\mathrm{r}} \tag{4}$$

where $\psi_\mathrm{m} = ||\boldsymbol{\psi}_\mathrm{m}||$ and the magnitudes of other vectors are obtained similarly. If needed, the iron losses can be taken into account separately (as described in the Appendix).

III. Saturation Models

A. Conventional Functions

Conventionally, the saturable magnetizing inductance is modeled as

$$L_\mathrm{m}(\psi_\mathrm{m}) = \frac{\psi_\mathrm{m}}{i_\mathrm{m}(\psi_\mathrm{m})} \quad \text{or} \quad L_\mathrm{m}(i_\mathrm{m}) = \frac{\psi_\mathrm{m}(i_\mathrm{m})}{i_\mathrm{m}} \tag{5}$$

The first form is often preferred since $i_\mathrm{m}(\psi_\mathrm{m})$ can be modeled using polynomials or power functions. For example, the power function [10], [5]

$$i_\mathrm{m}(\psi_\mathrm{m}) = \frac{\psi_\mathrm{m}}{L_{\mathrm{m}0}}\left(1 + \alpha\psi_\mathrm{m}^a\right) \tag{6}$$

includes only three parameters ($\alpha \geq 0$, $a \geq 0$, and the unsaturated inductance $L_{\mathrm{m}0} > 0$). The resulting inductance function is

$$L_\mathrm{m}(\psi_\mathrm{m}) = \frac{L_{\mathrm{m}0}}{1 + \alpha\psi_\mathrm{m}^a} \tag{7}$$

If needed, functions corresponding to (6) could be used to model $i_\mathrm{r}(\psi_{\mathrm{r}\sigma})$ or $i_\mathrm{s}(\psi_{\mathrm{s}\sigma})$. This kind of saturation models always fulfill (4), but they cannot model the mutual saturation effect. Instead of the power function (6), a polynomial could be used [9], [7].

B. Proposed Power Function

In this paper, the mutual saturation effect is taken into account by modeling the magnetizing inductance L_m and the rotor leakage inductance $L_{\mathrm{r}\sigma}$ as

$$L_\mathrm{m}(\psi_\mathrm{m}, \psi_{\mathrm{r}\sigma}) = \frac{\psi_\mathrm{m}}{i_\mathrm{m}(\psi_\mathrm{m}, \psi_{\mathrm{r}\sigma})} \tag{8a}$$

$$L_{\mathrm{r}\sigma}(\psi_\mathrm{m}, \psi_{\mathrm{r}\sigma}) = \frac{\psi_{\mathrm{r}\sigma}}{i_\mathrm{r}(\psi_\mathrm{m}, \psi_{\mathrm{r}\sigma})} \tag{8b}$$

In operating points typical of controlled induction motor drives, the stator leakage inductance $L_{\mathrm{s}\sigma}$ can usually be assumed to be a constant [3]. Due to these assumptions, only the reciprocity condition

$$\frac{\partial i_\mathrm{m}}{\partial\psi_{\mathrm{r}\sigma}} = \frac{\partial i_\mathrm{r}}{\partial\psi_\mathrm{m}} \tag{9}$$

is needed.

The goal is to find physically reasonable functions $i_\mathrm{m}(\psi_\mathrm{m}, \psi_{\mathrm{r}\sigma})$ and $i_\mathrm{r}(\psi_\mathrm{m}, \psi_{\mathrm{r}\sigma})$ fulfilling (9) and having a small number of parameters. It is convenient to consider functions of the form [15]

$$i_\mathrm{m}(\psi_\mathrm{m}, \psi_{\mathrm{r}\sigma}) = i'_\mathrm{m}(\psi_\mathrm{m}) + \frac{\mathrm{d}f(\psi_\mathrm{m})}{\mathrm{d}\psi_\mathrm{m}}g(\psi_{\mathrm{r}\sigma}) \tag{10a}$$

$$i_\mathrm{r}(\psi_\mathrm{m}, \psi_{\mathrm{r}\sigma}) = i'_\mathrm{r}(\psi_{\mathrm{r}\sigma}) + f(\psi_\mathrm{m})\frac{\mathrm{d}g(\psi_{\mathrm{r}\sigma})}{\mathrm{d}\psi_{\mathrm{r}\sigma}} \tag{10b}$$

The function (6) is adopted for $i'_\mathrm{m}(\psi_\mathrm{m})$ and $i'_\mathrm{r}(\psi_{\mathrm{r}\sigma})$. The mutual saturation effect is modeled with power functions: $f(\psi_\mathrm{m}) \propto \psi_\mathrm{m}^{c+2}$ and $g(\psi_{\mathrm{r}\sigma}) \propto \psi_\mathrm{m}^{d+2}$.

The resulting saturation characteristics are

$$i_\mathrm{m}(\psi_\mathrm{m}, \psi_{\mathrm{r}\sigma}) = \frac{\psi_\mathrm{m}}{L_{\mathrm{m}0}}\left(1 + \alpha\psi_\mathrm{m}^a + \frac{\gamma L_{\mathrm{m}0}}{d+2}\psi_\mathrm{m}^c\psi_{\mathrm{r}\sigma}^{d+2}\right) \tag{11a}$$

$$i_\mathrm{r}(\psi_\mathrm{m}, \psi_{\mathrm{r}\sigma}) = \frac{\psi_{\mathrm{r}\sigma}}{L_{\mathrm{r}\sigma 0}}\left(1 + \beta\psi_{\mathrm{r}\sigma}^b + \frac{\gamma L_{\mathrm{r}\sigma 0}}{c+2}\psi_\mathrm{m}^{c+2}\psi_{\mathrm{r}\sigma}^d\right) \tag{11b}$$

where $\{\alpha, \beta, \gamma\} \geq 0$ and $\{a, b, c, d\} \geq 0$. It can be easily shown that the condition (9) holds. Furthermore, any other functions could be used for $i'_\mathrm{m}(\psi_\mathrm{m})$ and $i'_\mathrm{r}(\psi_{\mathrm{r}\sigma})$ without

violating the reciprocity condition. The inductances corresponding to (11) are

$$L_{\mathrm{m}}(\psi_{\mathrm{m}},\psi_{\mathrm{r}\sigma}) = \frac{L_{\mathrm{m0}}}{1+\alpha\psi_{\mathrm{m}}^{a}+\frac{\gamma L_{\mathrm{m0}}}{d+2}\psi_{\mathrm{m}}^{c}\psi_{\mathrm{r}\sigma}^{d+2}} \tag{12a}$$

$$L_{\mathrm{r}\sigma}(\psi_{\mathrm{m}},\psi_{\mathrm{r}\sigma}) = \frac{L_{\mathrm{r}\sigma 0}}{1+\beta\psi_{\mathrm{r}\sigma}^{b}+\frac{\gamma L_{\mathrm{r}\sigma 0}}{c+2}\psi_{\mathrm{m}}^{c+2}\psi_{\mathrm{r}\sigma}^{d}} \tag{12b}$$

If no mutual saturation existed in the machine to be analyzed, parameter γ would be zero and the model would be identical to the model proposed in [10].

IV. Parameter Identification

A. Direct Method

The currents and the fluxes of the machine can be calculated using FEA at different operating points. The parameters of the proposed model are fitted by minimizing the cost function

$$\begin{aligned} &J(L_{\mathrm{m0}},L_{\mathrm{r}\sigma 0},\alpha,\beta,\gamma,a,b,c,d) \\ &\quad=\sum_{n=1}^{N}\left(\hat{L}_{\mathrm{m},n}-L_{\mathrm{m},n}\right)^2+\left(\hat{L}_{\mathrm{r}\sigma,n}-L_{\mathrm{r}\sigma,n}\right)^2 \end{aligned} \tag{13}$$

where the magnetizing inductance is $L_{\mathrm{m}}=\psi_{\mathrm{m}}/i_{\mathrm{m}}$ and the rotor leakage inductance is $L_{\mathrm{r}\sigma}=\psi_{\mathrm{r}\sigma}/i_{\mathrm{r}}$. The inductance estimates $\hat{L}_{\mathrm{m}}$ and $\hat{L}_{\mathrm{r}\sigma}$ are calculated from (12) using the actual values of the fluxes ψ_{m} and $\psi_{\mathrm{r}\sigma}$ in each operating point. The index n refers to an operating point and N is the total number of different operating points.

B. Indirect Method

The inductances of the induction machine cannot be measured directly. However, the parameters of the inductance functions (12) can be identified indirectly based on more easily measurable variables: the stator voltage $\boldsymbol{u}_{\mathrm{s}}$, the stator current $\boldsymbol{i}_{\mathrm{s}}$, and the angular speed ω_{m} of the rotor. The identification method is based on steady-state measurements.

1) No-Load Test: First, the stator resistance R_{s} is measured. Then, the machine is operated in steady state at no load at various voltage levels. At each operating point, the estimate $\hat{\boldsymbol{\psi}}_{\mathrm{m}}$ of the main flux is determined based on the stator voltage equation (2a):

$$\hat{\boldsymbol{\psi}}_{\mathrm{m}} = -\mathbf{J}\left(\boldsymbol{u}_{\mathrm{s}}-R_{\mathrm{s}}\boldsymbol{i}_{\mathrm{s}}\right)/\omega_{\mathrm{s}}-\hat{L}_{\mathrm{s}\sigma}\boldsymbol{i}_{\mathrm{s}} \tag{14}$$

Considering (12a) at no load, the magnetizing inductance estimate can be expressed as

$$\hat{L}_{\mathrm{m}} = \frac{L_{\mathrm{m0}}}{1+\alpha\hat{\psi}_{\mathrm{m}}^{a}} \tag{15}$$

at every operating point. The main flux vector and the stator current vector are parallel, $\boldsymbol{\psi}_{\mathrm{m}}=L_{\mathrm{m}}\boldsymbol{i}_{\mathrm{s}}$, since the rotor current is zero. The cost function to be minimized is

$$J(\hat{L}_{\mathrm{s}\sigma},L_{\mathrm{m0}},\alpha,a)=\sum_{n=1}^{N}\left(\hat{L}_{\mathrm{m},n}-\hat{\psi}_{\mathrm{m},n}/i_{\mathrm{s},n}\right)^2 \tag{16}$$

2) Load Test: The parameters $\hat{L}_{\mathrm{s}\sigma}$, L_{m0}, α, and a are known after the no-load test. It was found that the exponents b, c, and d have a relatively small effect on the resulting saturation characteristics, but they make the fitting process more difficult. Therefore, it was decided to predetermine those parameters based on a priori information. Direct fitting to the FEA data of 2.2-kW and 37-kW machines gave $b=1\ldots1.5$, $c=1\ldots1.5$ and $d=0\ldots0.5$. To determine the remaining parameters of the inductance model (12), the motor is operated at various voltage levels and at various non-zero slip frequencies.

The main flux estimate $\hat{\boldsymbol{\psi}}_{\mathrm{m}}$ is evaluated independently of the inductance model (12) using the stator voltage equation (14). The rotor leakage flux estimate can be expressed as

$$\hat{\boldsymbol{\psi}}_{\mathrm{r}\sigma} = \frac{\hat{R}_{\mathrm{r}}}{\omega_{\mathrm{r}}}\mathbf{J}\left(\hat{\boldsymbol{i}}_{\mathrm{m}}-\boldsymbol{i}_{\mathrm{s}}\right)-\hat{\boldsymbol{\psi}}_{\mathrm{m}} \tag{17a}$$

where

$$\hat{\boldsymbol{i}}_{\mathrm{m}} = \frac{\hat{\boldsymbol{\psi}}_{\mathrm{m}}}{L_{\mathrm{m0}}}\left(1+\alpha\hat{\psi}_{\mathrm{m}}^{a}+\frac{\gamma L_{\mathrm{m0}}}{d+2}\hat{\psi}_{\mathrm{m}}^{c}\hat{\psi}_{\mathrm{r}\sigma}^{d+2}\right) \tag{17b}$$

in accordance with (11a). At each operating point, the rotor leakage flux estimate $\hat{\boldsymbol{\psi}}_{\mathrm{r}\sigma}$ can be numerically[1] solved from (17) for any given values of $\hat{R}_{\mathrm{r}}$ and γ. Then, the inductance estimates corresponding to (12) can be evaluated:

$$\hat{L}_{\mathrm{m}} = \frac{L_{\mathrm{m0}}}{1+\alpha\hat{\psi}_{\mathrm{m}}^{a}+\frac{\gamma L_{\mathrm{m0}}}{d+2}\hat{\psi}_{\mathrm{m}}^{c}\hat{\psi}_{\mathrm{r}\sigma}^{d+2}} \tag{18a}$$

$$\hat{L}_{\mathrm{r}\sigma} = \frac{L_{\mathrm{r}\sigma 0}}{1+\beta\hat{\psi}_{\mathrm{r}\sigma}^{b}+\frac{\gamma L_{\mathrm{r}\sigma 0}}{c+2}\hat{\psi}_{\mathrm{m}}^{c+2}\hat{\psi}_{\mathrm{r}\sigma}^{d}} \tag{18b}$$

Based on the rotor voltage equation (2b), the rotor inductance can be expressed as

$$L_{\mathrm{r}} = \frac{R_{\mathrm{r}}\boldsymbol{i}_{\mathrm{s}}^{\mathrm{T}}\mathbf{J}\boldsymbol{\psi}_{\mathrm{r}}}{\omega_{\mathrm{r}}\boldsymbol{i}_{\mathrm{s}}^{\mathrm{T}}\boldsymbol{\psi}_{\mathrm{r}}} \tag{19}$$

The values for $\hat{R}_{\mathrm{r}}$, $L_{\mathrm{r}\sigma 0}$, β, and γ are obtained by minimizing

$$J(\hat{R}_{\mathrm{r}},L_{\mathrm{r}\sigma 0},\beta,\gamma)=\sum_{n=1}^{N}\left(\hat{L}_{\mathrm{r}}-\frac{\hat{R}_{\mathrm{r}}\boldsymbol{i}_{\mathrm{s},n}^{\mathrm{T}}\mathbf{J}\hat{\boldsymbol{\psi}}_{\mathrm{r},n}}{\omega_{\mathrm{r},n}\boldsymbol{i}_{\mathrm{s},n}^{\mathrm{T}}\hat{\boldsymbol{\psi}}_{\mathrm{r},n}}\right)^2 \tag{20}$$

where the rotor inductance estimate is $\hat{L}_{\mathrm{r}}=\hat{L}_{\mathrm{m}}+\hat{L}_{\mathrm{r}\sigma}$ and the rotor flux estimate is $\hat{\boldsymbol{\psi}}_{\mathrm{r}}=\hat{\boldsymbol{\psi}}_{\mathrm{m}}+\hat{\boldsymbol{\psi}}_{\mathrm{r}\sigma}$. It is worth noticing that there are alternative ways to indirectly identify the parameters of the inductance model; the method described above is comparatively robust against measurement errors.

V. Results

Saturation characteristics of a 2.2-kW squirrel-cage induction machine were studied by means of two-dimensional time-harmonic FEA [16], [4] and laboratory experiments. The machine is equipped with closed and skewed rotor slots, and its rating is: voltage 400 V; current 5 A; frequency 50 Hz; speed 1436 r/min; and torque 14.6 Nm. The base values are: angular frequency $2\pi 50$ rad/s; voltage $\sqrt{2/3}\cdot 400$ V; and current $\sqrt{2}\cdot 5$ A.

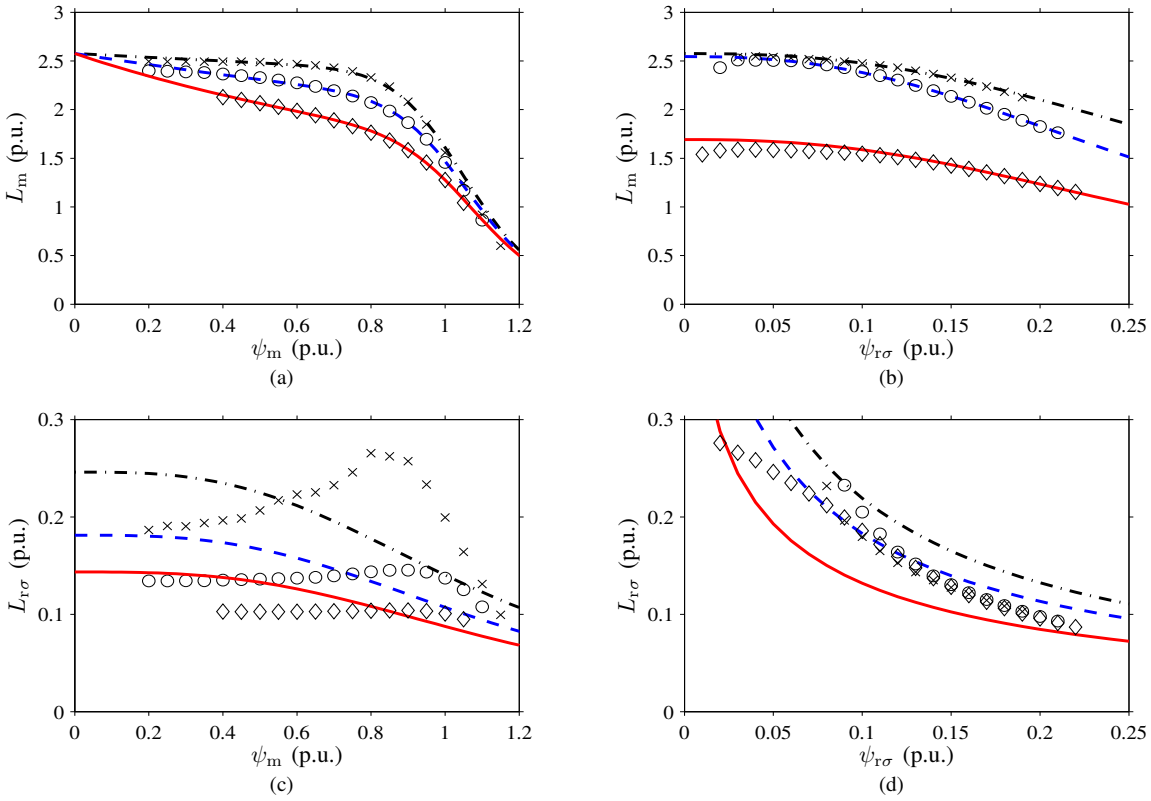

Fig. 4. Results of direct method applied to the inductance values obtained from the FEA data: (a) L_m as a function of ψ_m for three different values of $\psi_{\mathrm{r}\sigma}$, (b) L_m as a function of $\psi_{\mathrm{r}\sigma}$ for three different values of ψ_m, (c) rotor leakage inductance $L_{\mathrm{r}\sigma}$ as a function of ψ_m for three different values of $\psi_{\mathrm{r}\sigma}$, (d) $L_{\mathrm{r}\sigma}$ as a function of $\psi_{\mathrm{r}\sigma}$ for three different values of ψ_m. In (a) and (c), the values of $\psi_{\mathrm{r}\sigma}$ correspond to $i_\mathrm{r} \approx 0.5$ p.u. (dash-dotted line), $i_\mathrm{r} \approx 1.0$ p.u. (dashed line) and $i_\mathrm{r} \approx 2.0$ p.u. (solid line). In (b) and (d), the values of ψ_m are 0.4 p.u. (dash-dotted line), 0.7 p.u. (dashed line) and 1.0 p.u. (solid line).

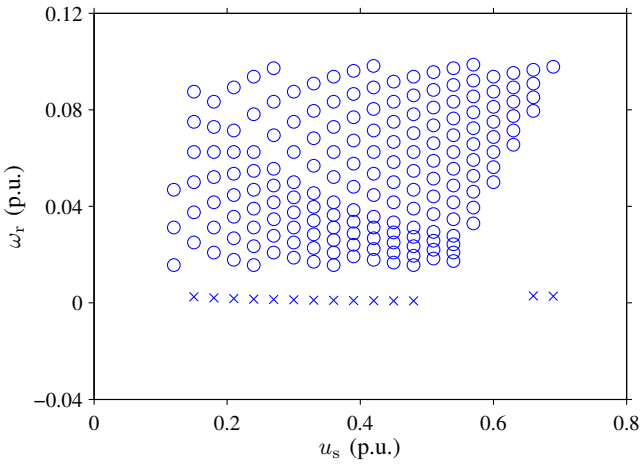

Fig. 3. Stator voltage magnitudes and angular slip frequencies used in parameter estimation from the FEA data. Circles denote the data used in load tests, crosses denote the no-load data. The stator frequency is 0.5 p.u.

TABLE I
FITTED PER-UNIT PARAMETERS OBTAINED FROM FEA DATA AND EXPERIMENTAL DATA

	FEA Direct	FEA Indirect	Experimental
$L_{\mathrm{m}0}$	2.58	2.57	2.27
$L_{\mathrm{r}\sigma 0}$	0.691	1.23	0.365
$L_{\mathrm{s}\sigma}$	-	0.0224	0.0270
R_r	-	0.0398	0.0395
α	0.523	0.445	0.459
β	20.1	37.9	22.1
γ	30.6	30.2	20.4
a	10.5	10.0	7.5
b	1.0	1.0	1.0
c	1.0	1.0	1.0
d	0.5	0.5	0.5

A. Finite Element Analysis

The operating points used in parameter estimation from the FEA data are presented in Fig. 3. The stator frequency ω_s was 0.5 p.u. The no-load points were not used in direct fitting.

1) Direct Method: The parameters of the proposed model (12) were identified based on the inductance data obtained from FEA. The direct method presented in Section IV-A was used. Since fractional exponents may be computationally inefficient, the exponents a, b, c, and d were rounded to the nearest half-integers (or integers) after the first fitting, and the other parameters were re-fitted. The fitted per-unit parameters are given in Table I.

The inductance data from FEA and the curves from the fitted functions are shown in Fig. 4. In Fig. 4(a), the magnetizing inductance L_m is shown as a function of ψ_m for three different values of $\psi_{\mathrm{r}\sigma}$. In Fig. 4(b), L_m is shown as a function of $\psi_{\mathrm{r}\sigma}$ for three different values of ψ_m. Similar representation for the rotor leakage inductance $L_{\mathrm{r}\sigma}$ is used in Figs. 4(c) and 4(d).

[1]Analytical solution can be found if $d = 0$.

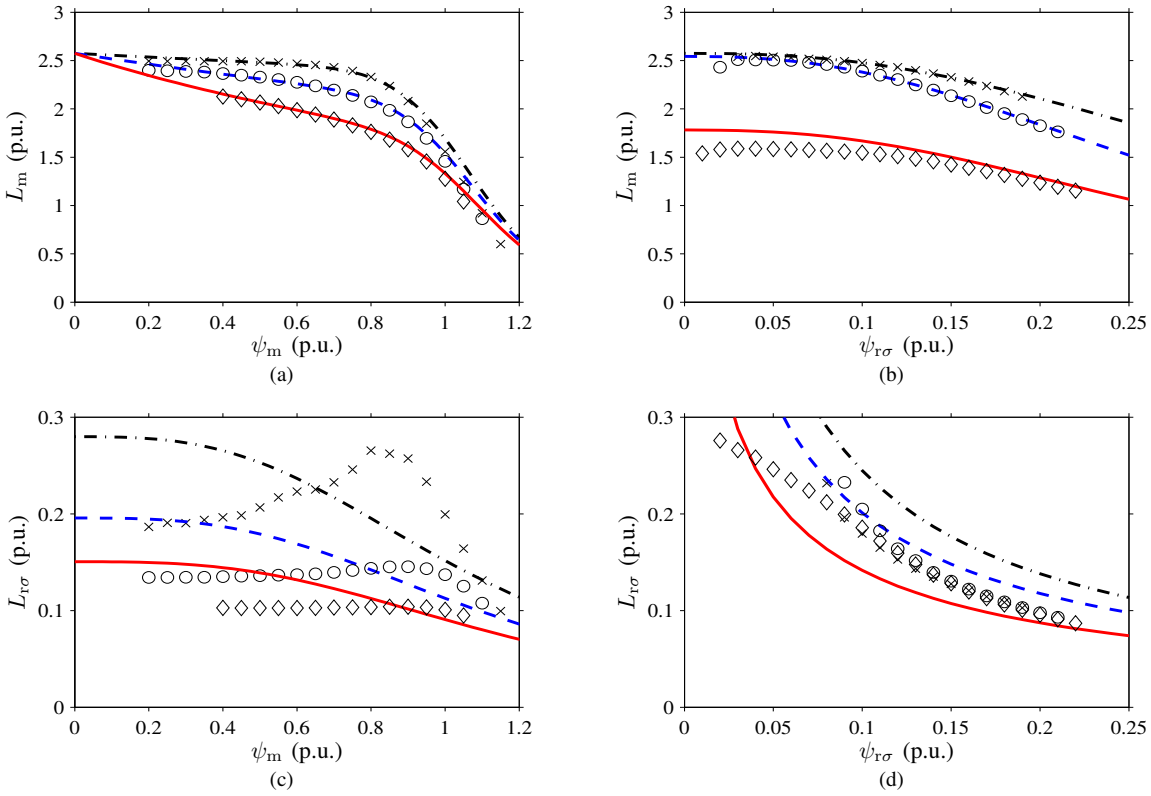

Fig. 5. Results of indirect method applied to the FEA data: (a) L_m as a function of ψ_m for three different values of $\psi_{\mathrm{r}\sigma}$, (b) L_m as a function of $\psi_{\mathrm{r}\sigma}$ for three different values of ψ_m, (c) $L_{\mathrm{r}\sigma}$ as a function of ψ_m for three different values of $\psi_{\mathrm{r}\sigma}$, (d) $L_{\mathrm{r}\sigma}$ as a function of $\psi_{\mathrm{r}\sigma}$ for three different values of ψ_m. In (a) and (c), the values of $\psi_{\mathrm{r}\sigma}$ correspond to $i_\mathrm{r} \approx 0.5$ p.u. (dash-dotted line), $i_\mathrm{r} \approx 1.0$ p.u. (dashed line) and $i_\mathrm{r} \approx 2.0$ p.u. (solid line). In (b) and (d), the values of ψ_m are 0.4 p.u. (dash-dotted line), 0.7 p.u. (dashed line) and 1.0 p.u. (solid line).

It can be seen that the proposed model for L_m fits very well to the FEA data. The mutual saturation appears to be very significant in the analyzed machine; in the case of no mutual saturation, the curves in Fig. 4(a) would overlap while the curves in Fig. 4(b) would be straight horizontal lines.

The differences in $L_{\mathrm{r}\sigma}$ between the FEA data and the fitted curves at low values of $\psi_{\mathrm{r}\sigma}$ are partly due to numerical problems in FEA; the rotor-side parameters cannot be determined reliably if the rotor current is close to zero. Furthermore, the peak in $L_{\mathrm{r}\sigma}$ in the vicinity of $\psi_\mathrm{m} \approx 0.8$ p.u. is not consistent with the reciprocity condition; there should be similar peak in L_m as a function of $\psi_{\mathrm{r}\sigma}$.

2) Indirect Method: The indirect method presented in Section IV-B is demonstrated by first applying it to the FEA data. The direct method applied to the 2.2-kW machine proposes the exponents $b = 1$, $c = 1$ and $d = 0.5$, hence these values were fixed. The stator resistance was fixed to R_s = 0.0779 p.u. based on the FEA data. The fitted per-unit parameters are given in Table I.

It can be noticed that the parameter values, particularly $L_{\mathrm{r}\sigma 0}$ and β, differ from those obtained by using the direct method. The assumption of constant stator leakage inductance has an effect on parameters α and a, whereas β and γ are affected by the assumption of constant rotor resistance.

The inductance data from FEA and the curves from the fitted functions are shown in Fig. 5 in a fashion similar to Fig. 4. The differences between the curves obtained by using the direct method (Fig. 4) and indirect method (Fig. 5) are small.

B. Experiments

In the laboratory experiments, the 2.2-kW induction machine was fed by a frequency converter. At each operating point, the stator frequency was $\omega_\mathrm{s} = 0.5$ p.u, while the magnitude of the stator voltage was varied. The slip frequency ω_r was adjusted using a servo motor.

The indirect method was used to identify the parameters of the inductance model based on experimental data. The stator resistance was fixed to R_s = 0.0628 p.u. obtained from a dc test. Before data fitting, the exponents $b = 1$, $c = 1$, and $d = 0.5$ were fixed, based on results from FEA data. The operating points used in indirect parameter estimation from the experimental data are presented in Fig. 7.

The resulting inductance values are depicted in Fig. 6 in a fashion similar to Figs. 4 and 5, and the fitted per-unit parameters are given in Table I. The behavior of the inductances is very similar to the results from FEA.

For comparison, the estimated and measured stator currents are depicted in Fig. 8. In Fig. 8(a), i_s is shown as a function of u_s for three different values of ω_r. In Fig. 8(b), i_s is shown as a function of ω_r for three different values of u_s. Similar representation for the displacement power factor $\cos\varphi$ is used in Figs. 8(c) and 8(d). The values of the stator current were obtained by inserting the stator voltage and the slip frequency into the motor model and finding the values for $\boldsymbol{\psi}_\mathrm{m}$ and $\boldsymbol{\psi}_{\mathrm{r}\sigma}$ that satisfied the voltage equations (2) in steady state.

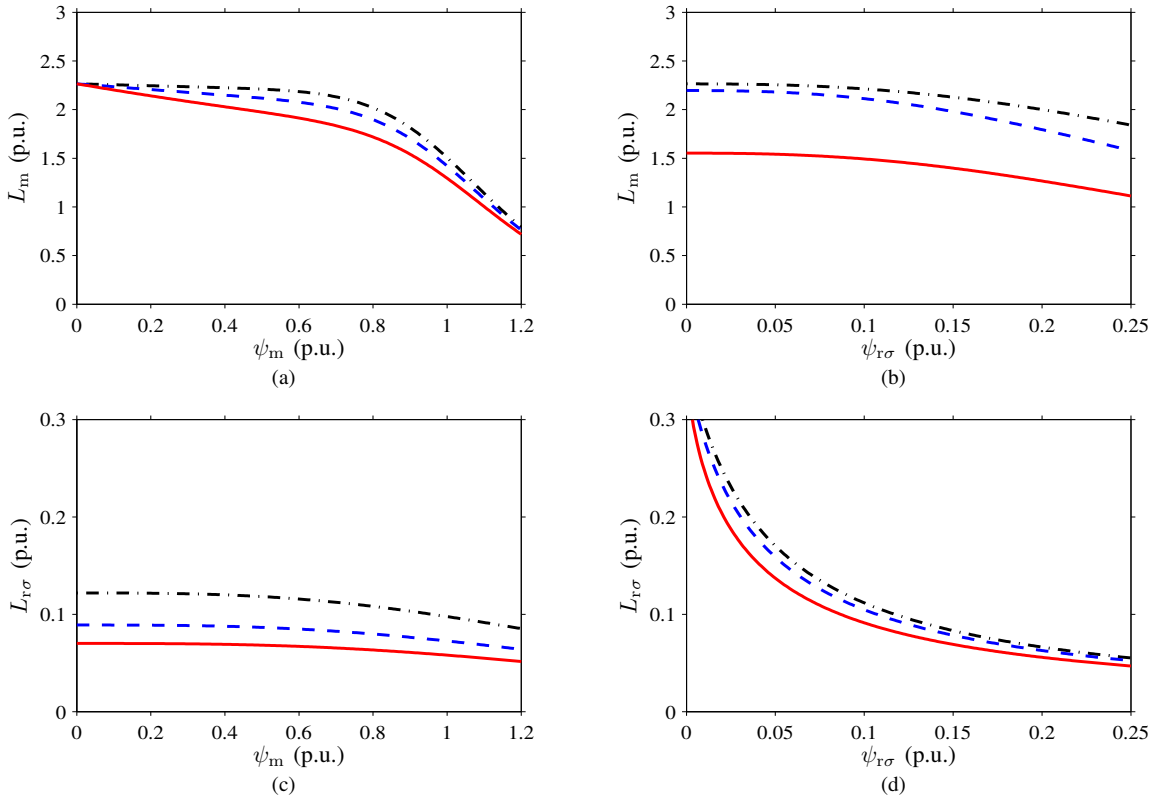

Fig. 6. Results of indirect method applied to experimental data: (a) L_m as a function of ψ_m for three different values of $\psi_{\mathrm{r}\sigma}$, (b) L_m as a function of $\psi_{\mathrm{r}\sigma}$ for three different values of ψ_m, (c) $L_{\mathrm{r}\sigma}$ as a function of ψ_m for three different values of $\psi_{\mathrm{r}\sigma}$, (d) $L_{\mathrm{r}\sigma}$ as a function of $\psi_{\mathrm{r}\sigma}$ for three different values of ψ_m. In (a) and (c), the values of $\psi_{\mathrm{r}\sigma}$ are 0.09 p.u. (dash-dotted line), 0.14 p.u. (dashed line) and 0.19 p.u. (solid line). In (b) and (d), the values of ψ_m are 0.4 p.u. (dash-dotted line), 0.7 p.u. (dashed line) and 1.0 p.u. (solid line).

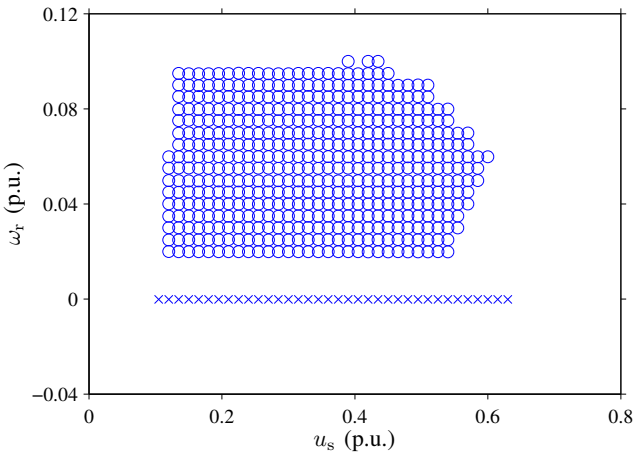

Fig. 7. Stator voltage magnitudes and angular slip frequencies used in indirect parameter estimation from the experimental data. Circles denote the data used in load tests, crosses denote the no-load data. The stator frequency is 0.5 p.u.

The model predicts the magnitude of the stator current and the displacement power factor with good accuracy. The error in the estimated displacement power factor originates from the assumptions made in the model (i.e. ignoring the iron losses, and using a constant rotor resistance).

VI. Conclusions

Mutual saturation between the main flux and the rotor leakage flux appearing in induction machines can be modeled analytically. The proposed functions are physically reasonable, they are easy to fit, and the number of their parameters is small. The functions can be used in real-time applications and in computer simulations where high accuracy and physical consistency are preferable. The model fits well to the magnetizing inductance data obtained from finite element analysis and experimental data for a 2.2-kW induction motor with closed and skewed rotor slots.

Appendix
Iron Losses

Fig. 9 illustrates the dynamic T model augmented with the stator-iron-loss resistance $R_{\mathrm{Fe,s}}$ [17], [18] and the stray-load-loss resistance $R_{\mathrm{Fe},\sigma}$ [19]. The losses related to constant $R_{\mathrm{Fe,s}}$ and $R_{\mathrm{Fe},\sigma}$ are proportional to $\omega_\mathrm{s}^2\psi_\mathrm{s}^2$ and $\omega_\mathrm{r}^2\psi_{\mathrm{r}\sigma}^2$, respectively, in steady state. If the inductance model is lossless (reciprocal), the power balance of the model is well defined. The proposed saturation models could be directly used in the model in Fig. 9.

Acknowledgment

This work was supported by the Finnish Funding Agency for Technology and Innovation, ABB Oy, Kone Oyj, and High Speed Tech Oy Ltd.

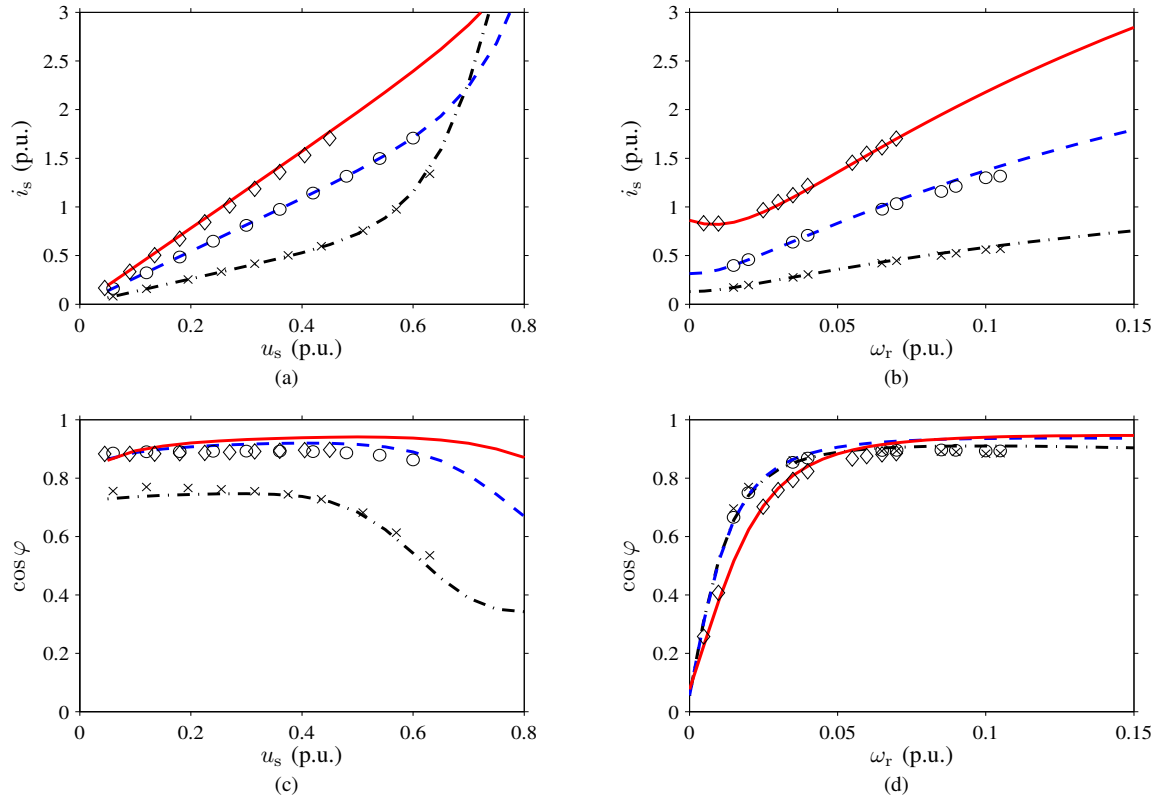

Fig. 8. Results of indirect method applied to experimental data: (a) magnitude of stator current i_s as a function of u_s for three different values of ω_r, (b) i_s as a function of ω_r for three different values of u_s, (c) displacement power factor $\cos\varphi$ as a function of u_s for three different values of ω_r, (d) $\cos\varphi$ as a function of ω_r for three different values of u_s. In (a) and (c), the values of ω_r are 0.02 p.u. (dash-dotted line), 0.06 p.u. (dashed line) and 0.1 p.u. (solid line). In (b) and (d), the values of u_s are 0.15 p.u. (dash-dotted line), 0.35 p.u. (dashed line) and 0.55 p.u. (solid line).

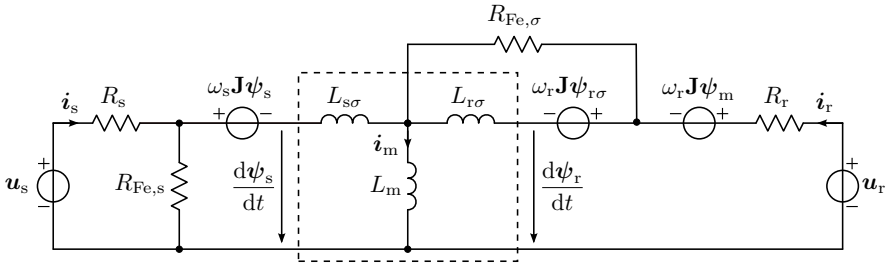

Fig. 9. Dynamic T model of Fig. 2 augmented with two iron loss resistances. Resistance $R_{Fe,s}$ is related to iron losses in the stator while $R_{Fe,\sigma}$ models the stray-load losses.

REFERENCES

[1] A. Yahiaoui and F. Bouillault, "Saturation effect on the electromagnetic behaviour of an induction machine," *IEEE Trans. Magn.*, vol. 31, no. 3, pp. 2036–2039, May 1995.

[2] C. Gerada, K. J. Bradley, M. Sumner, and P. Sewell, "Evaluation and modelling of cross saturation due to leakage flux in vector controlled induction machines," *IEEE Trans. Ind. Appl*, vol. 43, no. 3, pp. 694–702, May/June 2007.

[3] M. Hinkkanen, A.-K. Repo, and J. Luomi, "Influence of magnetic saturation on induction motor model selection," in *Proc. ICEM'06*, Chania, Greece, Sept. 2006, CD-ROM.

[4] A. Arkkio, "Analysis of induction motors based on the numerical solution of the magnetic field and circuit equations," Ph.D. dissertation, Dept. Elect. Commun. Eng., Helsinki Univ. Tech., Espoo, Finland, Dec. 1987. [Online]. Available: http://lib.tkk.fi/Diss/198X/isbn951226076X/

[5] N. R. Klaes, "Parameter identification of an induction machine with regard to dependencies on saturation," *IEEE Trans. Ind. Appl.*, vol. 29, no. 6, pp. 1135–1140, Nov./Dec. 1993.

[6] E. Levi, "Main flux saturation modelling in double-cage and deep-bar induction machines," *IEEE Trans. Energy Convers.*, vol. 11, no. 2, pp. 305–311, June 1996.

[7] S. D. Sudhoff, D. C. Aliprantis, B. T. Kuhn, and P. L. Chapman, "Experimental characterization procedure for use with an advanced induction machine model," *IEEE Trans. Energy Convers.*, vol. 18, no. 1, pp. 48–56, Mar. 2003.

[8] R. C. Healey, S. Williamson, and S. C. Smith, "Improved cage rotor models for vector controlled induction motors," *IEEE Trans. Ind. Appl.*, vol. 31, no. 4, pp. 812–822, July/Aug. 1995.

[9] J. A. Melkebeek and J. L. Willems, "Reciprocity relations for the mutual inductances between orthogonal axis windings in saturated salient-pole machines," *IEEE Trans. Ind. Appl.*, vol. 26, no. 1, pp. 107–114, Jan./Feb. 1990.

[10] H. C. J. de Jong, "Saturation in electrical machines," in *Proc. ICEM'80*, vol. 3, Athens, Greece, Sept. 1980, pp. 1545–1552.

[11] C. R. Sullivan and S. R. Sanders, "Models for induction machines with magnetic saturation of the main flux path," *IEEE Trans. Ind. Appl*, vol. 31, no. 4, pp. 907–917, July/Aug. 1995.

[12] M. Hinkkanen, A.-K. Repo, M. Cederholm, and J. Luomi, "Small-signal modelling of saturated induction machines with closed or skewed rotor slots," in *Conf. Rec. IEEE-IAS Annu. Meeting*, New Orleans, Louisiana,

Sept. 2007, pp. 1200–1206.
[13] M. Akbaba, M. Taleb, and A. Rumeli, "Improved estimation of induction motor parameters," *Electric Power Systems Research*, vol. 34, no. 1, pp. 65–73, July 1995.
[14] L. O. Chua, "Dynamic nonlinear networks: State-of-the-art," *IEEE Trans. Circuits Syst.*, vol. CAS-27, no. 11, pp. 1059–1087, Nov. 1980.
[15] A. Vagati, M. Pastorelli, F. Scapino, and G. Franceschini, "Impact of cross saturation in synchronous reluctance motors of the trasverselaminated type," *IEEE Trans. Ind. Appl.*, vol. 36, no. 4, pp. 1039–1046, Jul./Aug. 2000.
[16] J. Luomi, A. Niemenmaa, and A. Arkkio, "On the use of effective reluctivities in magnetic field analysis of induction motors fed from a sinusoidal voltage source," in *Proc. ICEM'86*, vol. 3, Munich, Germany, Sept. 1986, pp. 706–709.
[17] G. R. Slemon, "Modelling of induction machines for electric drives," *IEEE Trans. Ind. Appl.*, vol. 25, no. 6, pp. 1126–1131, Nov./Dec. 1989.
[18] S. Shinnaka, "Proposition of new mathematical models with core loss factor for controlling ac motors," in *Proc. IEEE IECON'98*, vol. 1, Aachen, Germany, Aug./Sept. 1998, pp. 297–302.
[19] E. Levi, A. Lamine, and A. Cavagnino, "Impact of stray load losses on vector control accuracy in current-fed induction motor drives," *IEEE Trans. Energy Convers.*, vol. 21, no. 2, pp. 442–450, June 2006.